An upper limit to [C II] emission in a $z \simeq 5$ galaxy

Gaelen Marsden,[1]* Colin Borys,[2] Scott C. Chapman,[2] Mark Halpern[1]
and Douglas Scott[1]

[1]*Department of Physics & Astronomy, University of British Columbia, 6224 Agricultural Rd, Vancouver BC, V6T 1Z1, Canada*
[2]*California Institute of Technology, 1201 East California Blvd, Pasadena CA, 91125, USA*

ABSTRACT

Low-ionization-state far-infrared (FIR) emission lines may be useful diagnostics of star formation activity in young galaxies, and at high redshift may be detectable from the ground. In practice, however, very little is known concerning how strong such line emission might be in the early Universe. We attempted to detect the 158-μm [C II] line from a lensed galaxy at $z = 4.926$ using the Caltech Submillimeter Observatory. This source is an ordinary galaxy, in the sense that it shows high but not extreme star formation, but lensing makes it visible. Our analysis includes a careful consideration of the calibrations and weighting of the individual scans. We find only a modest improvement over the simpler reduction methods, however, and the final spectrum remains dominated by systematic baseline ripple effects. We obtain a 95 per cent confidence upper limit of 33 mJy for a 200 km s^{-1} full width at half maximum line, corresponding to an unlensed luminosity of 1×10^9 L$_\odot$ for a standard cosmology. Combining this with a marginal detection of the continuum emission using the James Clerk Maxwell Telescope, we derive an upper limit of 0.4 per cent for the ratio of $L_{[C II]}/L_{FIR}$ in this object.

Key words: galaxies: evolution – galaxies: formation – galaxies: high-redshift – cosmology: observations – submillimetre.

1 INTRODUCTION

Low-ionization-state far-infrared (FIR) emission lines play an important role in cooling star-forming regions, and they allow us to infer the flux of rest-frame ultraviolet (UV) photons. Star-forming galaxies have large dust masses which obscure UV radiation, so we rely on the IR and longer wavelengths to probe these star-forming regions. Studies have shown that [C II], the ground-state fine-structure line of singly ionized carbon ($^2P_{3/2} \rightarrow \, ^2P_{1/2}$, $\lambda = 157.7409 \, \mu m$), is the dominant cooling line in gas-rich star-forming regions (Dalgarno & McCray 1972; Crawford et al. 1985; Stacey et al. 1991). It is thus expected to be a probe of star formation in young galaxies. In some nearby galaxies the [C II] line accounts for as much as 1 per cent of the far-IR luminosity (Stacey et al. 1991; Nikola et al. 1998; Mochizuki 2000). On the other hand, in some more distant ultraluminous infrared galaxies (ULIRGs) results from *ISO* indicated much lower fractions (Malhotra et al. 2001; Contursi et al. 2002; Luhman et al. 2003). At $z \simeq 5$ we know very little concerning the physical conditions within star-forming galaxies. Metallicity, UV flux, dust content and geometry could all be radically different

from that for more nearby (and hence cosmically older) systems. In the absence of much empirical data, even upper limits on [C II] luminosities are therefore worthwhile.

[C II] is the brightest line in our Galaxy (Mizutani et al. 1994), but its wavelength makes it impossible to observe from the ground. At high redshift, where the line is redshifted into the submillimetre range, there is great promise for using this line to probe early galaxy evolution, or even to find the first objects (e.g. Stark 1997; Suginohara, Suginohara & Spergel 1998). Until instruments with much wider back-ends and greatly improved sensitivity become available, progress can only be made slowly, by targeting individually promising objects.

The $z = 4.926$ lensed galaxy, detected as a red arc in the cluster CL 1358+62 (referred to as 'G1' in Franx et al. 1997, hereafter F97), magnified by a factor of 5–11, represents a particularly promising target for observing [C II] from the ground. Its redshift places the line at an accessible frequency ($\simeq 320$ GHz), though not ideal as it is on the edge of an atmospheric water line. The galaxy has a reasonably high inferred star formation rate ($\simeq 36$ M$_\odot$ yr^{-1}, F97), and unlike quasars observed at similar redshifts, the [C II] line is expected to be close to the systemic redshift of the galaxy. Moreover, although rest-frame UV colours indicate significant reddening, there is little submillimetre continuum detected, with a 3σ upper limit of 4 mJy (van der Werf et al. 2001, but see Section 4).

*E-mail: gmarsden@physics.ubc.ca

In the following paper we discuss the analysis and interpretation of our data. Section 2 briefly describes the observing programme. Section 3 describes the specifics of our analysis procedures. The results are presented in Section 4 and discussed in Section 5.

2 OBSERVATIONS

Object G1 was targeted with the Caltech Submillimeter Observatory (CSO), located at 13 300 feet on the summit of Mauna Kea in Hawaii, over three nights in 1998 January. The telescope is a 10.4 m $f/0.4$ submillimetre antenna with an alt-az mount.

The atmospheric transmission during the observing run, as measured by the CSO τ meter at 225 GHz, was very good. The optical depth ranged from $\tau_{225} \simeq 0.03$ to 0.07, corresponding to an optical depth at 320 GHz of 0.32–0.55.

2.1 Frequency centre

F97 determined the redshift of G1 from the detection of Ly α emission at 7204 Å, giving $z = 4.926$. They note, however, that the Ly α line is asymmetric and that the measured Si II absorption line is blueshifted by $\sim$300 km s^{-1}. These features can be explained by an outflow model, whereby an expanding shell of neutral and ionized material absorbs the blue side of the Ly α line (e.g. Lequeux et al. 1995). We assume that the [C II] emission would be somewhere between the Ly α and Si II lines, and therefore centred the detector shifted $\Delta v \approx 200$ km s^{-1} from the Ly α centre, or $z = 4.922$. This is a reasonable assumption, as this shift is typical of linewidths observed in local galaxies. The [C II] emission line is redshifted to $\nu_0 = 320.939$ GHz for the expected centre of our source.

2.2 Instrumentation

Based on the calculations of the previous section, it is clear that the CSO 345-GHz receiver is the appropriate detector. This receiver is a single side-band SIS mixer with 1-GHz IF, and acousto-optical spectrometer (AOS) backends. For our observations the signals from the mixer were sent to three spectrometers simultaneously, with 50-, 500- and 1500-MHz bandwidths.

From the F97 detection of Si II in CL 1358+62-G1, we assume the [C II] line is $\simeq$200 km s^{-1} wide, corresponding to 200 MHz at our observing frequency. We therefore concentrate our efforts on data from the 1500-MHz receiver, use the 500-MHz data as a check and ignore the 50-MHz data.

On the first night the receivers were centred on the nominal line centre, 320.939 GHz. In an attempt to avoid confusing any systematic detector response with the shape of the emission line, the receiver was shifted by $\Delta v = 129.8$ km s^{-1} for the second and third nights.

The secondary mirror chop throw was set to 60 arcsec at 1.123 Hz on the first night. It was apparent that after observations of one night we had reached near the instrumental noise limit, so we set more conservative chop parameters, 40 arcsec at 0.7 Hz, on the second and third nights in an attempt to probe systematic effects. By changing the chop throw, we additionally decrease the probability of inadvertently chopping on to a nearby source.

2.3 Pointing and calibration

The telescope was pointed at $\alpha = 13^{\rm h} 59^{\rm m} 39\overset{s}{.}0$, $\delta = 62° 30' 47''$. This position was determined by visually comparing the *Hubble Space Telescope* (*HST*) image presented in F97 with coordinates of

Table 1. Details of observations. Row 1 shows the line centre of the receiver on each night. The rest of the table displays the number of usable scans taken on each night in each detector.

Night:		1	2	3
Receiver centre (GHz):		320.939	320.800	320.800
1500 MHz	Source scans:	142	236	42
	Calibr. scans:	42	71	10
500 MHz	Source scans:	142	236	42
	Calibr. scans:	41	75	10

cluster members published by Luppino et al. (1991), as F97 did not publish coordinates for G1. This process is accurate to within a few arcsec, which is well within the CSO beamsize at this frequency ($\simeq$20 arcsec). Pointing calibrations were performed occasionally throughout each night, using the ^{12}CO (3 $\rightarrow$ 2) line of IRC 10216.

Temperature and frequency calibrations were also performed several times throughout each observing session. Hereafter, 'calibration scan' refers to the temperature calibrations, i.e. spectra of a hot load, while 'source scan' refers to spectra of our source, G1.

In all, $\sim$ 450 usable source scans were acquired, simultaneously in each of the 500- and 1500-MHz detectors. Exact numbers are given in Table 1. The 1σ rms per raw scan is $\sim$40–80 mK.

3 ANALYSIS

CSO spectroscopic data are usually analysed using the CLASS (Continuum Line Analysis Single-dish Software, Buisson et al. 1995) software package. In the expectation that any detection would be at very low signal-to-noise ratio, we developed our own analysis procedures in order to maximize our control over the reduction process. In this section we describe our methods of calibration and reduction.

3.1 Calibration

CSO data are calibrated in real time by referring each source scan to the previous hot load calibration scan. Visual inspection of the 500- and 1500-MHz calibration scans show apparently unstable baselines, so we investigate whether a more careful calibration will result in lower noise.

We compare the mean value of each calibration scan to the variance of the following source scans and to the atmospheric opacity, τ_{225}. We find that the 500- and 1500-MHz calibration means and the source scan variances all correlate well, and that they track τ (see Fig. 1).

We propose three possible methods of calibrating the data: (i) for each source scan, use the most recent calibration scan (the CSO default); (ii) naively average together all calibration scans within each night; and (iii) interpolate each calibration channel in time across each night. The data are thus reduced, as described in Section 3.2, using each of the three calibration methods. Taking the variance in the final reduced scan as a measure, we find that method (ii) is clearly inferior to (i), while (i) and (iii) are not significantly different. We choose method (iii) as the most elegant solution. If baseline variations did not dominate the error budget, we might expect method (iii) to yield the best results, and we would advocate its use in general for low signal-to-noise ratio data.

3.2 Data reduction

The data are co-added within each night. First, a zeroth-order baseline, fit to the wings of the spectrum, is subtracted from each source
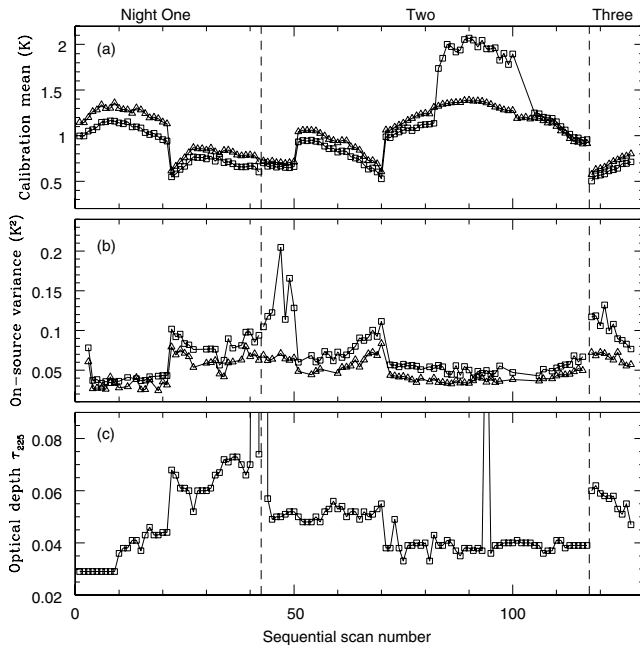
Figure 1. Trends in data as a function of time: (a) is the mean value of each calibration scan for both the 1500- (squares) and 500-MHz (triangles) spectrometers, measured in K; (b) is the variance of the source scans for both spectrometers, in K^2; (c) is the optical depth measured at 225 GHz with the CSO τ meter. Note the correlation between all three panels. The vertical dashed lines indicate the divisions between the three nights.

scan in order to minimize the effects of baseline drift. The data are then combined as a weighted average in each channel. Because of small shifts in the velocity centres and spacing throughout each night, we interpolate the data to a common set of velocity bins before averaging.

The summed scans for each night are binned into roughly 40 km s^{-1} wide channels, and the nights are averaged, weighted by the variance in each bin. We rebin the data to six different bin sizes and centres, and find no significant difference in the final result due to the choice in binning.

Finally, the co-added spectrum is converted from antenna temperature to flux density. The beam size and efficiency for the 345-GHz receiver are 24.6 arcsec and 74.6 per cent, respectively, (Kooi 2001). The resulting spectrum is shown in Fig. 2.

4 RESULTS

It is clear from Fig. 2 that the error bars are much smaller than the structure in the final spectrum. The systematics in the instrument prevent integrating down to such low noise levels. We re-estimate the error bars by finding the best-fitting Gaussian and scaling the errors so that $\chi^2 = N$, where N is the number of degrees of freedom in the fit.

A full four-parameter Gaussian fit will not converge to a meaningful result, so we instead fix the line centre and width to the a priori expected values of $v_0 = 0$ km s^{-1} and full width at half maximum (FWHM) = 200 km s^{-1} (as described in Section 2.1), and calculate the baseline as the weighted average of the data outside $\pm 2\sigma$ of the line centre. We find a 95 per cent upper limit of 33 mJy using the 1500-MHz receiver; the 500-MHz receiver gives consistent, although less constraining results. To convert from specific flux S_ν to luminosity L, we first integrate over frequency,
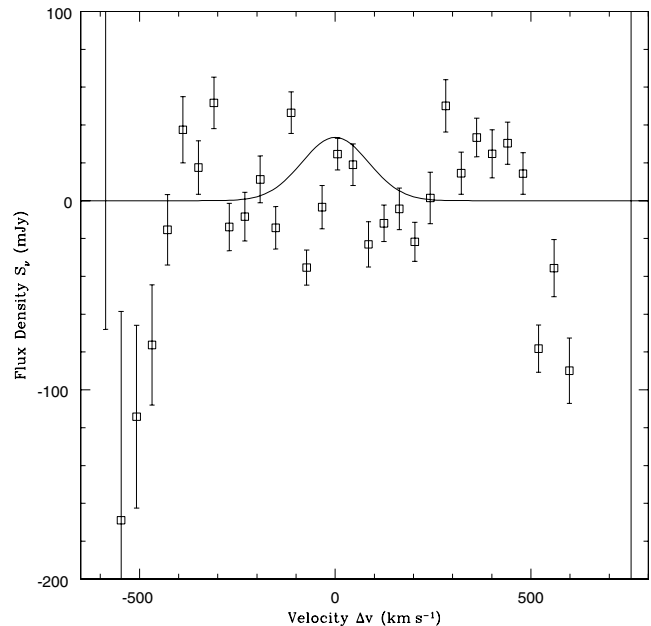
Figure 2. The co-added source spectrum, using data from the 1500-MHz detector. Error bars indicate statistical errors, calculated as the standard deviation of the data in each bin. The spectrum is dominated by baseline ripples. The solid curve is the 95 per cent upper limit for the [C II] emission line centred at $v = 0$ km s^{-1} (320.939 GHz) and with FWHM = 200 km s^{-1}.

$S = \int S_\nu \, d\nu = 1.06 \, S_\nu^{\text{peak}} \times$ FWHM for a Gaussian of height S_ν^{peak} and width FWHM = $\nu_0(\Delta v/c)$, then multiply by $4\pi D_L^2$, where D_L is the luminosity distance for a given cosmology. For a standard cosmological model with $\Omega_M = 0.3$, $\Omega_\Lambda = 0.7$ and $H_0 = 70$ km s^{-1} Mpc^{-1}, we find $D_L = 45.8$ Gpc and $L_{\text{[C II]}} = 5.4 \times 10^9$ L$_\odot$.

We also rereduce existing SCUBA observations at 850 μm (Holland et al. 1999) to find an estimate of the total FIR luminosity, L_{FIR}. An 850-μm upper limit of $S_\nu < 4$ mJy was reported by van der Werf et al. (2001) based on 4 ks of pointed photometry data. We combine 15 ks of jiggle-map data (∼2.5 mJy rms) with the photometry data (∼1.5 mJy rms) using the methods described in Borys et al. (2003) and find a 2.1σ peak 2 arcsec from G1, well within the 15-arcsec beam. Although not highly significant, and in a blank field survey we would not consider a 2σ peak a detection, this is a pointed measurement of a known source, so we consider this a measurement rather than simply an upper limit. We can then calculate the ratio $L_{\text{[C II]}}/L_{\text{FIR}}$ using Gaussian probability distributions to describe both $L_{\text{[C II]}}$ and L_{FIR}. Integrating a grey-body model with $T_{\text{dust}} = 40$ K and $\beta = 1.5$ (Combes 1999; Klaas et al. 2001) from 8 to 1000 μm, we then find that the SCUBA measurement $S_{850} = (2.8 \pm 1.3)$ mJy corresponds to $L_{\text{FIR}} = (2.4 \pm 1.2) \times 10^{12}$ L$_\odot$, assuming the same cosmology as above. Integrating over the joint probability, we find a Bayesian 95 (99) per cent upper limit $L_{\text{[C II]}}/L_{\text{FIR}} < 0.4$ (1.1) per cent.

5 DISCUSSION

Typical values of $L_{\text{[C II]}}/L_{\text{FIR}}$ are thought to be ∼0.1–1 per cent, but there is recent evidence to suggest that it can be lower, especially for ULIRGs, which are thought to make up a large fraction of the high-redshift submillimetre population. We find $L_{\text{[C II]}}L_{\text{FIR}} < 0.4$ per cent at 95 per cent confidence for our particular target. While this does not rule out the ratios found by Stacey et al. (1991), it does

confine the ratio for this particular high-redshift galaxy to the lower end of the range.

Based on their lensing model, F97 determine that the source G1 is magnified by a factor of 5–11. Taking the lower end of this magnification range, we find an unlensed luminosity of $L_{\rm [CII]} < 1 \times 10^9$ L$_\odot$. We can use the absolute $L_{\rm [CII]}$ measurement to place an upper limit on the star formation rate (SFR) occurring in the source. Boselli et al. (2002) relate SFR to $L_{\rm [CII]}$ by assuming an initial mass function, with slope $\alpha = 2.35$ of between 0.1 and 100 M$_\odot$, and using their [C II]–Hα relation determined from observations of a sample of Virgo galaxies, finding

$$\text{SFR} = 1.73 \times 10^{-6} \times (L_{\rm [CII]}/{\rm L}_\odot)^{0.788}\, {\rm M}_\odot\, {\rm yr}^{-1}.$$

Assuming this relation holds for all galaxies at all redshifts, and that the source is not differentially lensed, we find SFR $\lesssim$ 21 M$_\odot$ yr^{-1}. However, we note that Boselli et al. (2002) claim the relation only holds up to $10^{10.5}$ L$_\odot$ and that the SFR is uncertain by up to a factor of 10, so we should not place too much confidence in the estimate. As a comparison, F97 find SFR $\simeq$ 36 M$_\odot$ yr^{-1}, based on near-infrared photometry and the star formation model by Bruzual & Charlot (1993). Hence the SFR implied by our [C II] upper limit is loosely consistent with that inferred from the optical. However, given the approximations and assumptions made here, it is hard to draw any firm conclusions.

Luhman et al. (2003) find a deficit of [C II] ($L_{\rm [CII]} < 10^{-3}\, L_{\rm FIR}$) in a sample of ULIRGs, and claim a negative correlation between $L_{\rm [CII]}/L_{\rm FIR}$ and $L_\nu(60\,\mu{\rm m})/L_\nu(100\,\mu{\rm m})$ for galaxies of all types (see fig. 5 in Luhman et al. 2003). In order to compare our limit with sources in this plot, we calculate

$$L'_{\rm FIR} = 1.26 \times 10^{12} \times [2.58\, L_\nu(60\,\mu{\rm m}) + L_\nu(100\,\mu{\rm m})],$$

with L_ν evaluated at rest-frame wavelengths (assuming a modified blackbody) in W Hz^{-1} and $L'_{\rm FIR}$ in W (see Helou et al. 1988). We find $L_{\rm [CII]}/L'_{\rm FIR} < 4.4 \times 10^{-3}$ and $L_\nu(60\,\mu{\rm m})/L_\nu(100\,\mu{\rm m}) = 0.88$, which is consistent with the published relation for normal star-forming galaxies. Nevertheless, firmer upper limits at similar levels for a sample of high-redshift star-forming galaxies will help to determine if there is a difference in the role of [C II] in the early Universe.

Bolatto, Di Francesco & Willott (2004) recently reported an upper limit to $L_{\rm [CII]}/L_{\rm FIR}$ in a $z = 6.42$ quasar, observed with the JCMT. They find $L_{\rm [CII]}/L_{\rm FIR} < 5 \times 10^{-4}$. While this limit is lower than that published here, we note that a quasar is not a normal galaxy, and this source is ~200 brighter than ours, with $L_{\rm bol} \sim 10^{14}$ L$_\odot$. Our measurement, because of lensing amplification, has allowed us to place a useful limit in a single high-redshift star-forming galaxy. Clearly, this is a difficult programme, and more sensitive measurements of both the [C II] line emission and the FIR are required to significantly improve the constraint on $L_{\rm [CII]}/L_{\rm FIR}$.

REFERENCES

Bolatto A. D., Di Francesco J., Willott C. J., 2004, ApJ, 606, L101
Borys C., Chapman S., Halpern M., Scott D., 2003, MNRAS, 344, 385
Boselli A., Gavazzi G., Lequex J., Pierini D., 2002, A&A, 385, 454
Bruzual A. G., Charlot S., 1993, ApJ, 405, 538
Buisson G. et al., 1995, http://www.iram.fr/IRAMFR/GS/class/class.html
Combes F., 1999, Ap&SS, 269, 405
Contursi A. et al., 2002, AJ, 124, 751
Crawford M. K., Genzel R., Townes C. H., Watson D. M., 1985, ApJ, 291, 755
Dalgarno A., McCray R. A., 1972, ARA&A, 10, 375
Franx M., Illingworth G. D., Kelson D. D., van Dokkum P. G., Tran K., 1997, ApJ, 486, L75 (F97)
Helou G. et al., 1988, ApJS, 68, 151
Holland W. S. et al., 1999, MNRAS, 303, 659
Klaas U. et al., 2001, A&A, 379, 823
Kooi J. W., 2001, http://www.submm.caltech.edu/cso/receivers/beams.html (online reference only)
Lequeux J., Kunth D., Mas-Hesse J. M., Sargent W. L. W., 1995, A&A, 301, 18
Luhman M. L., Satyapal S., Fischer J., Wolfire M. G., Sturm E., Dudley C. C., Lutz D., Genzel R., 2003, ApJ, 594, 758
Luppino G. A., Cooke B. A., M$^{\rm c}$Hardy I. M., Ricker G. R., 1991, AJ, 102, 1
Malhotra S. et al., 2001, ApJ, 561, 766
Mizutani K. et al., 1994, ApJS, 91, 613
Mochizuki K., 2000, A&A, 363, 1123
Nikola T., Genzel R., Herrmann F., Madden S. C., Poglitsch A., Geis N., Townes C. H., Stacey G. J., 1998, ApJ, 504, 749
Stacey G. J., Geis N., Genzel R., Lugten J. B., Poglitsch A., Sternberg A., Townes C. H., 1991, ApJ, 373, 423
Stark A. A., 1997, ApJ, 481, 587
Suginohara T., Suginohara M., Spergel D. N., 1998, Mem. Soc. Astron. Italiana, 69, 447
van der Werf P. P., Knudsen K. K., Labbé I., Franx M., 2001, in Lowenthal J. D., Hughes D. H., eds, Proc. UMass/INAOE Conf. World Scientific, Singapore, p. 103

This paper has been typeset from a T$_{\rm E}$X/L$^{\rm A}$T$_{\rm E}$X file prepared by the author.